Desalination and Water Treatment
www.deswater.com

doi:10.5004/dwt.2019.23658

145 (2019) 337–347
March

Synthesis, characterization and adsorption of endrin on composite materials based on metal organic co-ordination complexes and zeolite

Ayub Nosheen*, Rafique Uzaira

Department of Environmental Sciences, Faculty of Sciences, Fatima Jinnah Women University, Rawalpindi, Pakistan, email: nosheen.ayub@gmail.com (A. Nosheen), uzairaiqbal@yahoo.com (R. Uzaira)

Received 19 June 2018; Accepted 20 December 2018

ABSTRACT

Hybrid coordination complex of MOF-199 [Cu_3 $(BTC)_2$] on zeolite was synthesized, characterized, and explored for the removal of endrin from waste water. For this purpose, upon hydrothermal crystallization of zeolite particles, MOF-199 from its synthetic solution was grown using solvothermal method. A range of techniques like XRD, FTIR and SEM/EDX were employed to determine the surface and bulk characteristics of synthesized materials. XRD exhibited the characteristic reflections of MOF-199 suggesting it as major component and further crystal lattice of parent MOF-199 remains intact in composite. FTIR results also witnessed co-existence of vibrational bands of both zeolite and MOF-199 confirming successful incorporation in the composite. EDX showed atomic weight percentage of zeolite (Si and Al) in ratio of 2.25% and 1.33% respectively with 11.24% Cu doped in MOF-199. The application of each synthesized material for adsorption studies of pesticide (endrin) in batch mode was analyzed on UFLC-UV under different parameters of concentration and dose as a function for 60 min. The results revealed maximum uptake (91%) of endrin on MOF-199@ZH, followed by 85% and 75% on MOF-199 and zeolite, respectively. Experimental data depicted good agreement for pseudo-second order kinetics and Langmuir adsorption isotherms with R^2 of 0.999.

Keywords: Endrin; Adsorption; MOF; Zeolite; Pesticide; Langmuir isotherm

1. Introduction

Water is utmost irreplaceable resource on earth for survival of living organisms. But fresh water accessibility is reducing constantly. This is due to constant pollution of water resources which affect quality of water. The deprived quality of water is not only disturbing human health but also affect other social and commercial activities [1]. Water pollution due to pesticides residue especially, chlorinated pesticides, is a crucial sustainability challenge [2]. And their existence of in the environment is of great concern due to their persistent nature and chronic adverse effect on human health and the environment [3–5]. All over the world, organochlorine pesticides have been extensively used in agricultural fields in order to increase the crop yield and control vector borne diseases [6,7]. Whereas various organochlorine pesticides have been banned in the developed countries but in some countries they are still in used especially Africa [8].

Pakistan's economy is mainly agro-based with 70% population directly related to agriculture, whereas 68% industrial business is linked with agriculture. To fulfill the increasing demand of food, use of pesticides and fertilizers has been increased 100 times in Pakistan during 1980–2002 [9]. A significant proportion (69%) of total pesticides is applied mainly on cotton crop; rest of pesticides is used for maize, wheat, rice, etc. [10]. Further, number of pesticide sprays that is almost 10 per crop is another drastic hazard to human health [11]. Organochlorine pesticides are in common use and they remain in the environment for long time after application. Organochlorine pesticides are classified into diphenylaliphatic, cyclodiene, chlorinated benzene and cyclohexane class. Endrin belongs to cyclodiene group that is applied on maize, rice, cotton and wheat crops [12], and bioaccumulation results in adverse effects in human population. Furthermore, headache, nausea, vomiting, con-

*Corresponding author.

vulsions and inhibition of neurotransmitter hormone as side effects of these pesticides is also reported [13,14].

The discharge of pesticide residues to water reservoirs is of great concern. Scientists are in continuous effort to develop different methods for removal of pesticides to maintain water quality. Adsorption is considered as one of the best wastewater treatment methods due to its wide range of applications and ease of operation [15]. Activated carbon is the most widely used adsorbent for the removal of organic pollutants from water due to high degree of porosity and an extensive surface area. However, it is found that the pore utility and adsorption capacity for large molecules is limited due to its microporous nature [16]. And also adsorption rate is much lower in natural water than in a single-solute adsorption system in pure water, because activated carbon usually removes not only the target contaminant but also natural organic matters [17], which prove that activated carbon generally has poor selectivity to organic pollutants. Moreover, activated carbon needs to be regenerated frequently during the adsorption process, which causes excessive mass loss and brings inconvenience to the operation procedures [18,19]. Consequently, it is attractive to develop novel adsorbents for removing organic micro-pollutants from water.

The present investigation is an attempt to use MOF-199@zeolite composite for the removal of Endrin from waste water through adsorption on individual and composite material. This is significant as MOF composite using zeolite as substrate offers a new dimension in the field of synthesis [20,21].

2. Experimental

The chemicals were obtained from Sigma-Aldrich and used without further purification. The significant reagents used were aluminum isopropoixde, tetraethyl ammonium hydroxide (TEAOH), tetra-ethyl-ortho-silicate (TEOS), trimesic acid or 1,3,5-benzene tri-carboxylic acid (TMA). The general chemicals of analytical reagent grade employed were ammonium nitrate (NH_4NO_3), sodium hydroxide (NaOH), copper nitrate hemipentahydrate ($Cu(NO_3)_2{\cdot}2.5H_2O$), methanol (CH_3OH), and N-N-dimethyl-formamide (DMF).

2.1. Synthesis of zeolite

For the synthesis of zeolite, adopted method [22] involved modification, where tetrapropyl ammonium bromide was replaced by tetraethyl ammonium hydroxide (TEAOH) as surfactant. This selection was based on the preference since TEAOH is a better templating agent that reduces crystallization period and facilitates to attain fully crystalline phase [23]. The general procedure (see Fig. 1) follows mixing of 0.1 g aluminum-isopropoxide in 1 M NaOH aqueous solution. The surfactant TEAOH solution (5 mL) was slowly added with continuous stirring till complete dissolution. The silica source TEOS (6 mL) was added in above solution and stirred again for 30 min to get a homogenous gel. Later, this gel was transferred to stainless steel autoclave and placed in furnace at 150°C at 10°C/min for 2 d. The crude material obtained was cooled, collected by centrifugation at 4000 rpm for 15 min, and washed repeatedly with deionized water. The product was dried in oven at 50°C and calcined at 600°C for 6 h. The synthesized zeolite was coded as ZH.

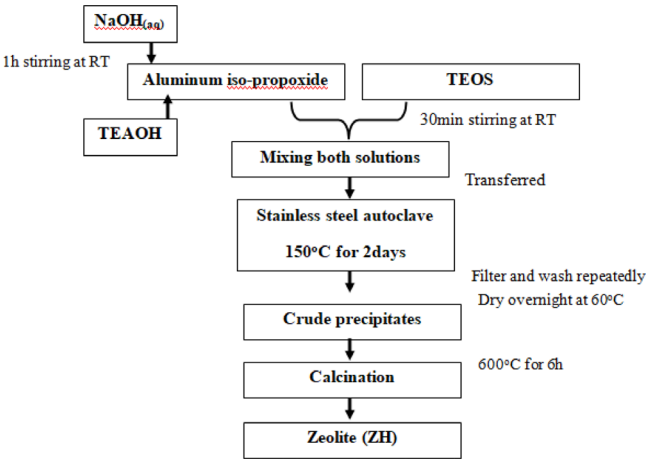

Fig. 1. Flow diagram of zeolite synthesis.

2.2. Synthesis of MOF-199

MOF-199 was synthesized based on trimesic acid as organic moiety with incorporation of copper metal following method reported by Thi et al. [24]. A brief summary of procedure is given (see Fig. 2).

0.368 g of copper nitrate hemipentahydrate was dissolved in 20 mL of DMF:CH_3OH:H_2O (1:1:1 v/v) with stirring. In a separate beaker, 0.148 g of trimesic acid (1,3,5-benzenetricarboxylic acid) was dissolved in 20 mL of the same solvent mixture. Both solutions are mixed and transferred to Teflon-lined autoclave for heating at 150°C for 24 h. The resulting precipitates obtained were collected by centrifugation and repeatedly washed with same solvent mixture and dried overnight in oven at 60°C.

2.3. Synthesis of MOF-199 @ZH composite

The work of Petit and Bandosz, 2010 [25] inspired the functionalization of zeolite with MOF for synthesis of composite in present research. The synthesis procedure is given below and also presented as flow chart (Fig. 3).

To the synthetic solution of MOF, 0.1 g of zeolite was suspended and heated in autoclave at 150°C for 24 h. After cooling to room temperature, the crude product obtained was washed repeatedly with chloroform and dried overnight in oven at 60°C. The composite synthesized was coded as MOF-199@ZH.

2.4. Characterization

For the characterization of synthesized materials, a number of techniques were employed. The finely grounded powdered samples were placed on a sample holder, and scanned from $2\theta = 5^o$–50^o with a step size of 0.0334° on X-ray diffraction XRD (X'Pert PRO MPD PANalytical diffractometer. The working conditions were Cu Kα radiation, λ = 1.5418 A°, voltage of 40kV and current of 40 mA. FTIR tech-

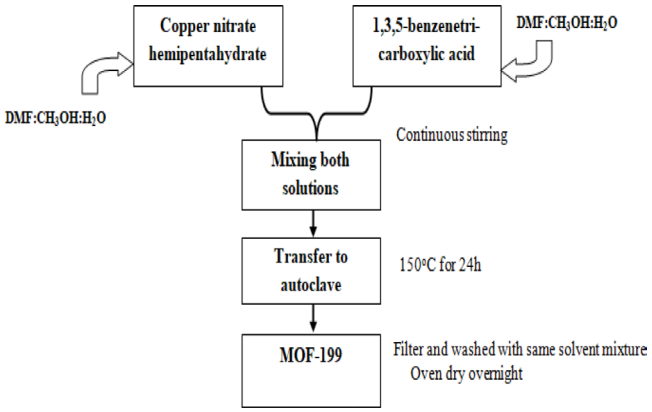

Fig. 2. Flow chart for synthesis of MOF-199.

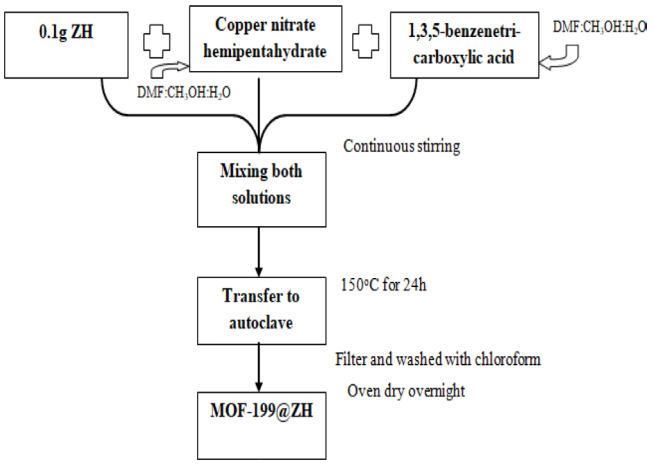

Fig. 3. Flow diagram for synthesis of MOF-199@ZH.

nique was used for the determination of functional groups in synthesized materials in transmittance (%) mode with a 16 cm^{-1} resolution and 50 scans in the mid IR region (400–4000 cm^{-1}). The morphology and elemental composition of prepared materials were examined on scanning electron microscope (Carl Zeiss Sigma, at 5 kV and 20 kV) coupled with EDX (Oxford Instrument X-Max 80).

2.5. Adsorption experiment

The synthesized materials (zeolite, MOF-199 and MOF-199@ZH) were subjected to analyze the removal of pesticide in batch mode. The effect of various parameters i.e. concentration (3, 5 and 7 mg/L), dose (5 and 10 mg) and pH (2–12) was studied with respect to time at room temperature (25°C).

The standard solution of adsorbate was prepared in n-hexane and an aliquot of 30, 50 and 70 mL was taken separately in 100 mL volumetric flask to prepare working solutions for studying the concentration effects. A known volume (10 µL) was injected into UFLC (LC-2010, Schimadzu) reverse phase HS-C18 column (250 mm 4.6 mm) equipped with UV detector. The solution was eluted at 0.5 mL/min with a solvent mixture of acetonitrile and water in 65:35 ratios, respectively and removal of endrin from sample solution was monitored. The amount of adsorption at equilibrium, q_e (mg/g) was calculated by Eqs. (1) and (2)

$$q_t = \frac{(C_i - C_t)V}{W} \tag{1}$$

$$q_e = \frac{(C_i - C_e)V}{W} \tag{2}$$

C_i, C_t and C_e (mg/L) is concentration of adsorbate at initial, at any time t and equilibrium, respectively. V is volume of solution in Liter and W is mass of adsorbent in g.

The percent removal of endrin from waste water was calculated using Eq. (3).

$$\%Removal = \frac{(C_i - C_t)}{C_i} \times 100 \tag{3}$$

2.6. Kinetic models and isotherms:

Different kinetic models (pseudo-first and pseudo-second order) and isotherms (Langmuir and Freundlich) were applied to investigate possible fitness of experimental data.

3. Result and discussion

Synthesis of MOF-199@ZH was carried out by hydrothermal crystallization of zeolite followed by solvothermal growth of MOF-199 from its synthetic solution in the presence of dispersed zeolite particles.

3.1. XRD analysis

XRD pattern of zeolite, MOF-199 and MOF-199@ZH is shown in Fig. 4. The reflection of zeolite (Fig. 4a) are consistent with reported topologies [26,27]. Characteristic reflections of MOF-199 (Fig. 4b) are observed at 2θ = 6.9°, 9.5°, 11.6°, 13.4°, 17.5°, 19.0° in good agreement with reported literature [28–30]. Furthermore, the composite (MOF-199@ZH) exhibits that main reflection of MOF-199 at 11.7° is not changed after modification. This suggests that MOF-199 is present as major component and preserve its crystalline character in the composite [31,32]. Thus, it is assumed that zeolite facilitates and acts as a bridge to link copper dimer and organic ligand [33].

3.2. FTIR spectroscopy

FTIR spectra (Fig. 5) show the characteristic asymmetric stretching vibration of T-O-T (T: Si or Al) in framework of zeolite [34] is at 1007 cm^{-1}. MOF-199 is characterized by typical bands centered around 1641/1552 cm^{-1} and 1453/1374 cm^{-1} corresponds to asymmetric and symmetric stretching vibrations of carboxylate group, respectively [35,36]. The presence of strong stretching vibration band at 1641.17 cm^{-1} confirms deprotonation of carboxylate in 1,3,5-benzenetricarboxylic acid upon reaction with metal ions [37,38]. The composite (MOF-199@ZH) also features five typical bands of MOF-199, suggesting significant contribution of the later in composite formation.

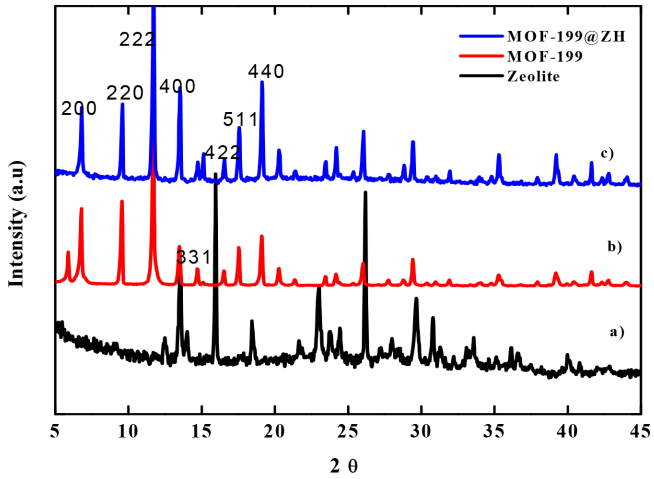

Fig. 4. XRD analysis of a) ZH, b) MOF-199 and c) MOF-199@ZH.

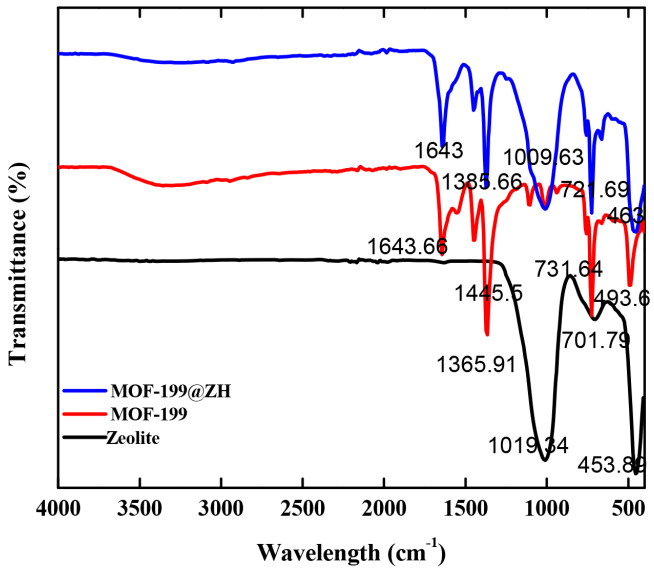

Fig. 5. FTIR spectrum of ZH, pure MOF-199 and MOF-199@ZH.

It is evident that vibration bands of zeolite and MOF-199 are in good agreement with published data [39]. Furthermore, all characteristic vibration bands of zeolite are also observed in MOF-199@ZH composite, indicating that composite was successfully synthesized with composition of zeolite and MOF-199. Hence it is concluded that FTIR spectra also confirm the results of XRD on the formation of zeolite, MOF-199 and composite material.

3.3. Scanning electron microscopy

SEM micrographs (see Fig. 6) present morphologies of zeolite, MOF-199 and composite. The zeolite is identified by pseudo-spherical forms constituted by small plates that form poly-crystal. Similar results are reported by Zubowa et al. [40] and (Rees and Chandrasekhar) [41]. On the other hand, solvothermal method for the synthesis of MOF-199 develops octahedral crystals. This is in accordance with

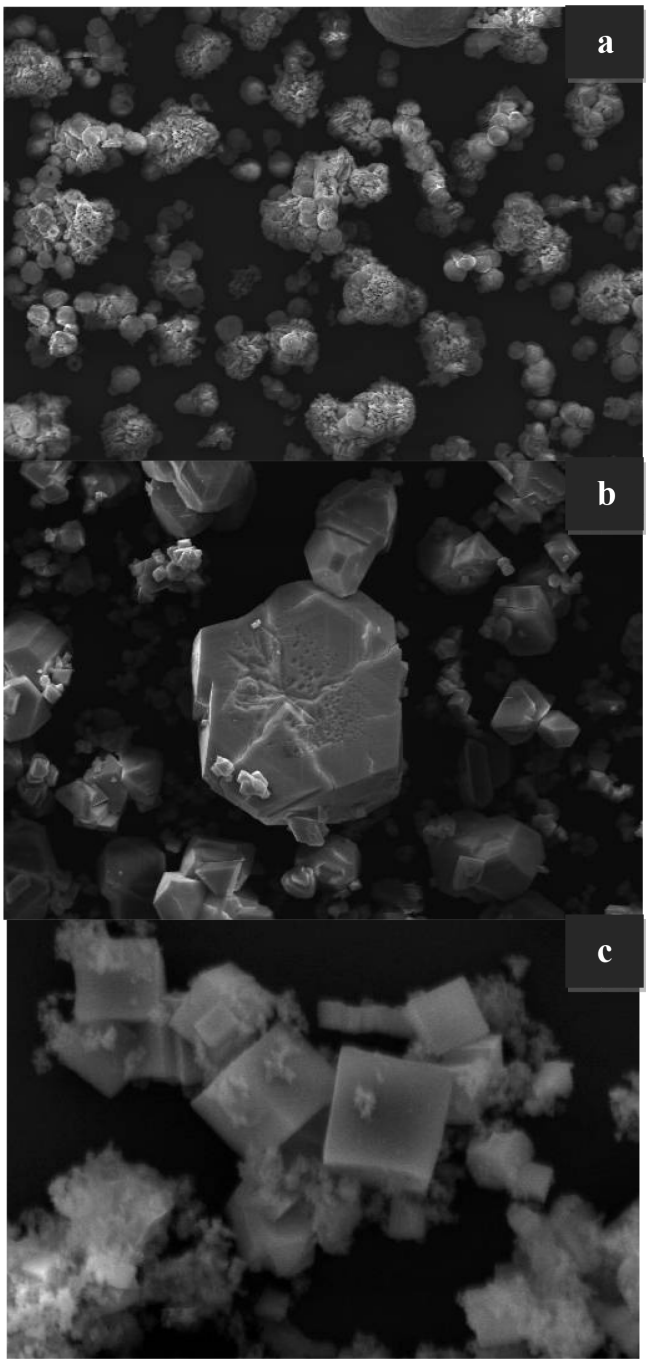

Fig. 6. SEM of a) ZH, b) MOF-199 and c) MOF-199@ZH.

reported literature [42]. A good combination of both morphologies (i.e, pseudo-spherical and octahedral) is found in composite. The retaining of host matrix intact is also witnessed by other researchers when zeolite is loaded with sample [43,44].

3.4. EDX spectroscopy

The results of EDX in tabular form and spectrum are presented in Table 1 and Fig. 7, respectively. As noted Si,

Table 1
Elemental weight percentage of synthesized materials

Elements / Materials ⇩ ⇨	O%	C%	Si%	Al%	Na%	Cu%
Zeolite	51.16	–	26.29	8.69	13.86	–
Cu-BTC	26.69	58.81	–	–	–	14.50
Cu-BTC@Z	37.46	47.71	2.25	1.33	–	11.24

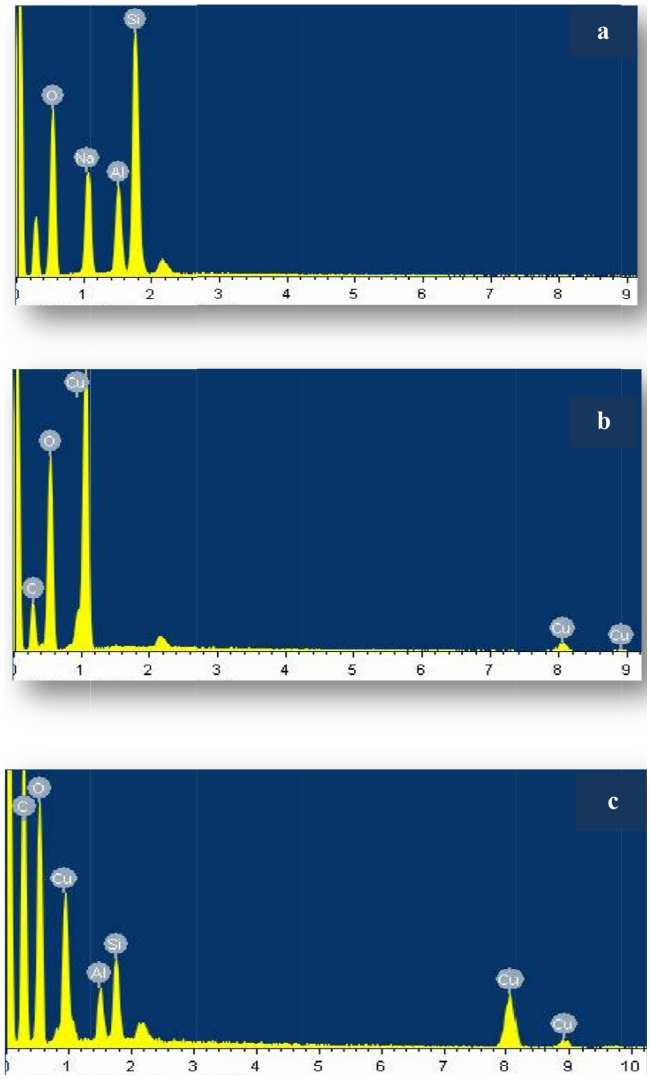

Fig. 7. EDX spectrum of a) ZH, b) MOF-199 and c) MOF-199@ZH.

Al and O are the construction elements with Kα characteristic X-ray energy of 1.739 KeV, 1.486 KeV and 0.525 KeV, respectively for zeolite. EDX of composite comprising of Si, Al, O and Cu peaks (see Fig. 7c), confirms presence of zeolite and MOF together. The primary construction element (Cu) in MOF-199 is observed at 2.042 KeV. It is to mention that 0 KeV represents instrumental base line.

The results conclude successful growth of zeolite onto MOF-199 and preservation of crystalline nature.

3.5. UFLC-UV analysis

Endrin is a commonly used organochlorine pesticide. Batch adsorption experiment was designed to study removal of endrin on synthesized material (zeolite, MOF-199 and MOF199@ZH) under varying parameters of time, pH of endrin, endrin concentration and adsorbent dose. The removal percentage was analyzed on Ultra Fine Liquid Chromatography (UFLC).

3.5.1. Effect of time

Adsorption of endrin using synthesized materials was carried out for 60 min batch mode. Fig. 8 shows the % removal and adsorption capacity of endrin at elevated time. The result shows that endrin uptake is rapid for the first 30 min and there after it proceeds at slow rate and finally remains constant. Same results are also reported on adsorption of pesticides on graphene oxide-magnetic nanoparticles [45]. The reason for increase in removal efficiency of endrin up to 30 min is due to an increase in number of vacant sites available at initial stage. While the repulsion forces between a guest molecule on the adsorbent surface and that in solution results in decrease in adsorption in later stages. Maximum removal is achieving by MOF-199@ZH composite which is up to 90% as compare to zeolite and MOF-199 (75 and 80% respectively). The higher removal of efficiency of endrin is obtain due to the hydrogen bonding between the oxygen atom of endrin molecules and carboxylic acid (–COOH) and hydroxyl (–OH) groups found on the surface of synthesized adsorbents (MOF-199, MOF-199@ZH and zeolite). Such trend is also reported on the adsorption of endrin on date stones [46].

3.5.2. Effect of adsorbate pH

The pH of adsorbate plays an important role in determining the extent of adsorption of substance on the surface of synthesized materials. For this, 5 mg/L of endrin is taken containing 10 mg of all adsorbents while maintaining the pH of adsorbate from 2.0 to 12.0 using 0.1 M NaOH and 0.1 M HCl. The solution mixture is agitated for 30 min of contact time at room temperature. Fig. 9 shows that a gradual increase in adsorption efficiency of endrin is obtained when pH of adsorbate is kept between 2.0 and 6.0 and get maximum adsorption at pH 6.0 followed by a gradual decrease. This is due to the hydrogen bonding between the oxygen atom of endrin molecules and carboxylic-acid (–COOH) and hydroxyl (–OH) groups found on the surface of MOF-199 and zeolite, respectively. However, adsorption rate of endrin on synthesized adsorbents decreases with the increase of pH due to dissociation of counter compounds in synthesized materials may increase resolution in a lower absorption of the given compound endrin. Same results are reported in literature [47–49].

3.5.3. Effect of adsorbate concentration

Batch adsorption study is also conducted by varying concentration (3 mg/L, 5 mg/L and 7 mg/L) at optimum dose (10 mg) for a specific time period (60 min).

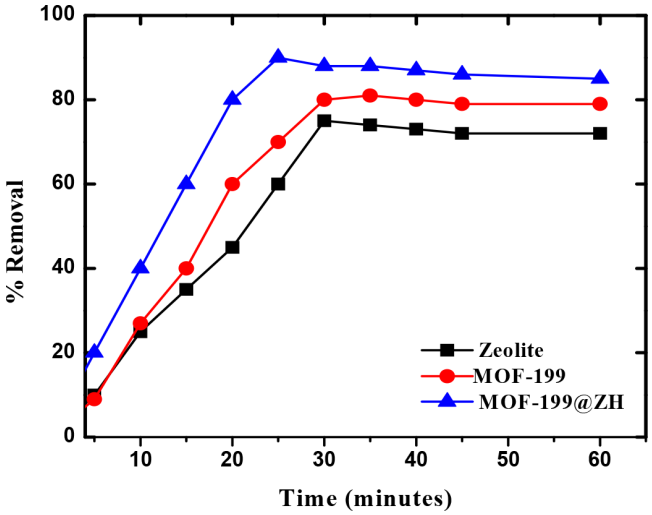

Fig. 8. Effect of time for the removal of Endrin with respect to (a) percentage and (b) adsorption capacity.

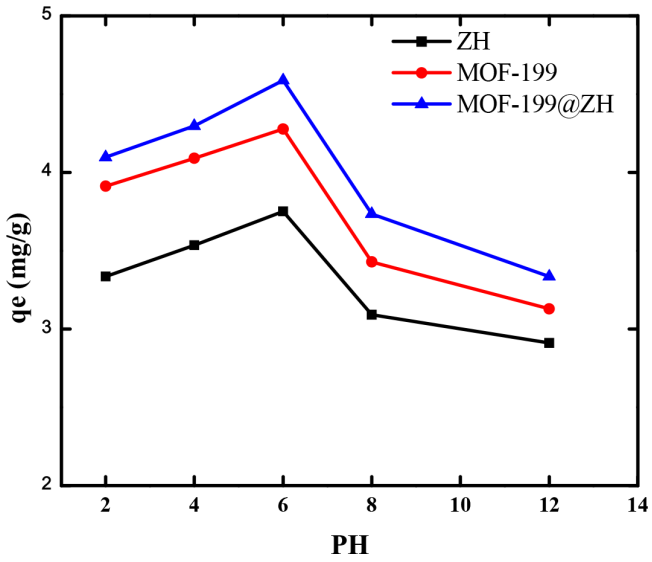

Fig. 9. Effect of adsorbate pH on adsorption capacity.

Fig. 10 shows the result for the effect of initial concentration (3–7 mg/L) on adsorption of endrin on synthesized materials. It is observed that endrin uptake increases and then decrease after increasing concentration up to 7 mg/L. This is due to the availability of many unoccupied sites on adsorbent surface, and when adsorbate concentration increases number of available active sites on adsorbent surfaces is reduced with attainment of the saturation point at 5 mg/L. Such results are reported in literature [50,51]. The equilibrium adsorption increases from 2 to 6 mg/mg, with an increase in the initial concentration increase from 3 to 7 mg/L (Fig. 11) and the equilibrium removal of endrin decrease from 69.7 to 64.26%, 79.98 to 75.87% and 86.16 to 78.96% on zeolite, MOF-199 and MOF-199@ZH composite, respectively. Maximum removal is observed at 5 mg/L by composite (91%) follows by MOF-199(86%) and zeolite (80%).

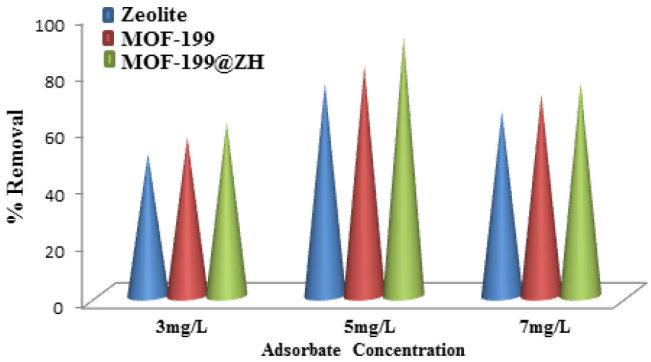

Fig. 10. Removal (% age) of endrin of with respect to adsorbate concentration.

3.5.4. Effect of adsorbent dose

The adsorbent dose also affects the adsorption and removal of target analyte form aqueous samples [52]. Therefore, the effect of dose is also studied on synthesize materials. Dose varies from 5–10 mg. Figs. 12 and 13 show the effect of adsorbent dose (mg) on the removal (% age) of endrin at C_o = 5 mg/L and 25°C. It shows that the removal of endrin increase with increase of dose up to 10 mg. At equilibrium time, the % removal increase from 60 to 91% for increase in dose from 5–10 mg. The increase in % removal is due to increase in available active sites. Similar trend is observed for all the synthesized adsorbent with maximum removal is shown by composite material (91%). The same results are reported in literature [53].

3.6. Kinetics and isotherms

Kinetic predicts the adsorption rate and gives important information for designing and modeling the adsorption processes. Eqs. (4) and (5) represent the linear equation for pseudo-first order [54] and pseudo-second order [55] model respectively.

$$\log\left(q_e - q_t\right) = \log q_e - \left(K_1 \mid 2.303\right)t \tag{4}$$

$$\frac{t}{q_t} = \frac{1}{K^2 q_e^{\,2}} + \frac{t}{q_e} \tag{5}$$

where q_e (mmol g^{-1}) is the amount of adsorbate (endrin) adsorbed at equilibrium and q_t (mmol g^{-1}) is consistent with the adsorption capacity at time t. Fitting supports the pseudo-second order reaction mechanism. k_1 (min^{-1}) is equal to the rate constant, determined by the plotting log ($q_e - q_t$) vs. t. k_2 (g mmol^{-1} min^{-1}) is the rate constant of pseudo-second-order kinetics. The slope and intercept of plot log($q_e - q_t$) or t/q_t versus t are used to calculate the pseudo-first or second-order rate constant k and q_e, respectively. Based on pseudo-second-order model, the calculated equilibrium adsorption (q_e) amount of endrin on MOF-199@ZH was approached to the value measured in experiments which is much more than that of zeolite and MOF-199, implying that MOF-199@ZH composites may play a vital role in enhancing adsorption capacity for endrin. Mean-

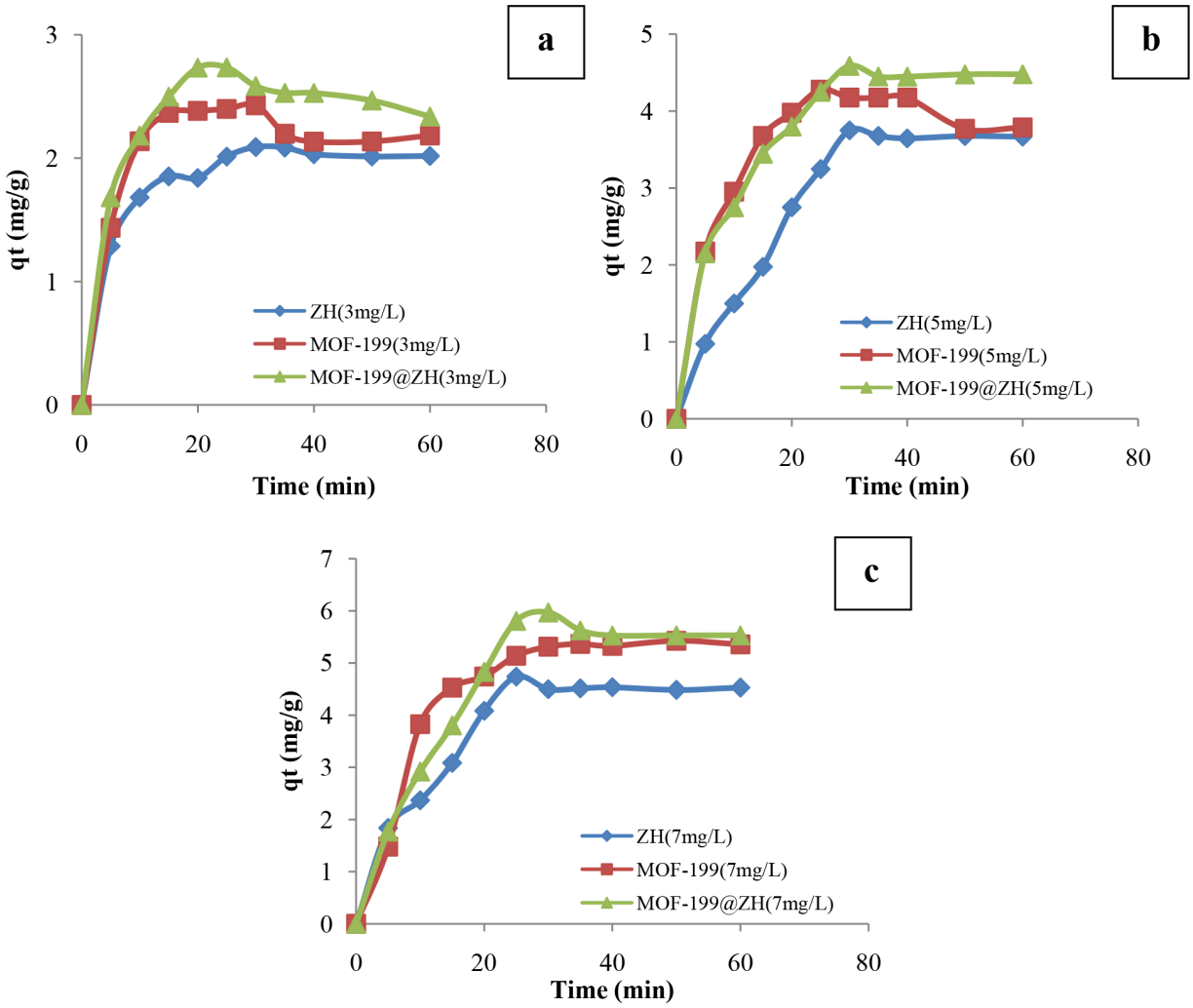

Fig. 11. Adsorption capacity with respect to adsorbate concentration at (a) 3 mg/L (b) 5 mg/L and (c) 7 mg/L.

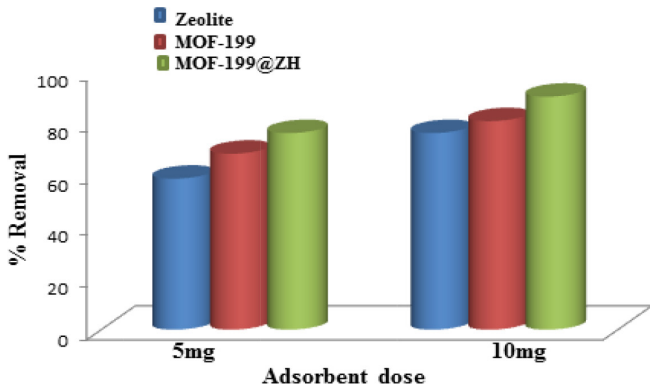

Fig. 12. Removal (% age) with respect to adsorbent dose.

while, the pseudo-second order model is properly fitted with the kinetic data by presenting high R^2 values represented in Table 2. It is suggested that the adsorption process of endrin on MOF-199@ZH can be described by the pseudo-second-order, which implies the adsorption rate depends on the concentration of function sites of MOF-199@ZH. Furthermore, the high R^2 value has been observed for the endrin adsorption on zeolite and MOF-199, indicating that the adsorption process also follows the pseudo-second-order kinetic model. The data fitted well with pseudo-second-order model also demonstrates that the limiting step of adsorption rate is chemisorption (i.e., valence forces) from the molecules share or exchange electrons between MOF-199@ZH and endrin [56].

The specific relationship between the equilibrium adsorbate concentration in the bulk and the amount adsorbed at the surface can be revealed by sorption isotherms. The isotherm results for endrin adsorption onto zeolite and MOF-199 and MOF-199@ZH at a room temperature were analyzed using two common isotherms, the Langmuir and Freundlich, The Langmuir isotherm [57] is expressed in the following equation.

$$\frac{C_e}{q_e} = \frac{1}{q_o} C_e + \frac{1}{K_L q_o} \tag{6}$$

C_e is the amount of un-adsorbed adsorbate concentration in solution at equilibrium (mg L^{-1}), q_o is the maximum

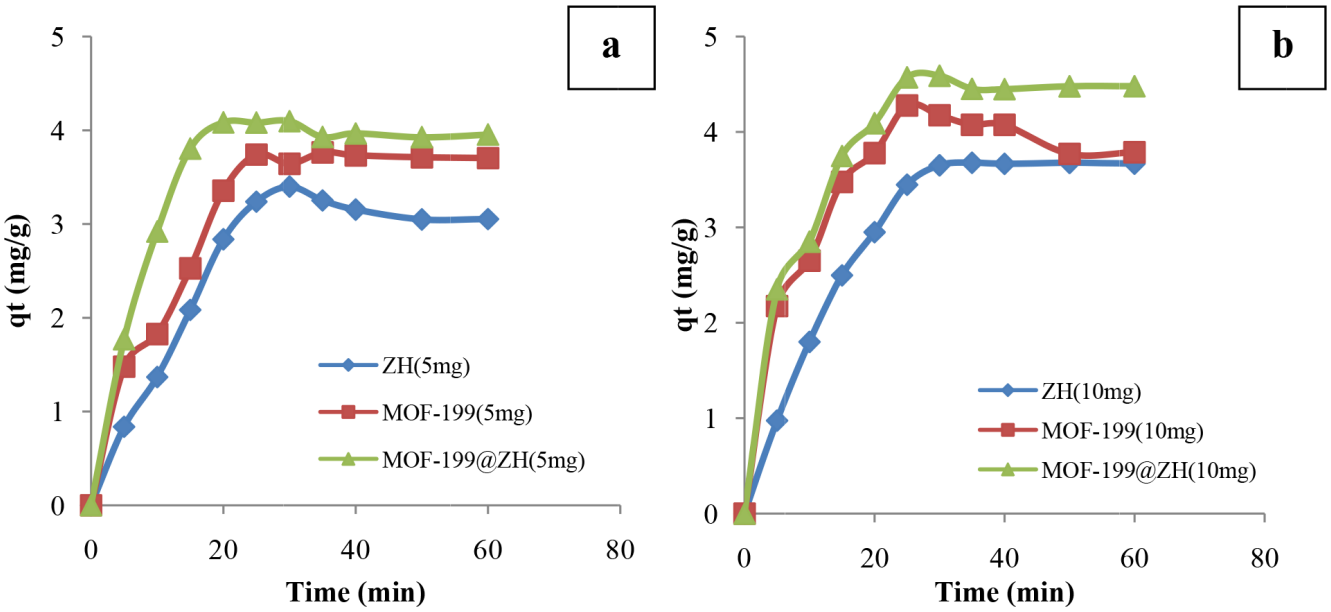

Fig. 13. Adsorption capacity with respect to adsorbent dose at (a) 5 mg dose (b) 10 mg dose.

Table 2
Pseudo-second order model of MOF-199@ZH

Adsorbent	Pseudo-second order model		
	K_2	q_e	R^2
	(g mg^{-1} min^{-1})	(mg g^{-1})	
Zeolite	1.916	1.91	0.9993
MOF-199	1.579	1.634	0.9995
MOF-199@ZH	1.307	2.549	0.9999

Table 3
Langmuir and Freundlich Isotherm of MOF-199@ZH

Adsorbent	Langmuir isotherm			Freundlich isotherm		
	q_o (mg g^{-1})	K_L (L mg^{-1})	R^2	K_f (mg g^{-1}) (L·mg^{-1})$^{1/n}$	$1/n$	R^2
Zeolite	5.659	1.23	0.9976	4.748	0.6129	0.9328
MOF-199	6.587	1.98	0.9985	3.879	0.8115	0.9787
MOF-199@ZH	7.861	2.18	0.9998	6.183	0.6933	0.9883

amount of adsorbate per unit mass of adsorbent to form a complete monolayer on the surface (mg g^{-1}), and k_L is a constant related to the affinity of the binding sites (L mg^{-1}). A linear plot of specific adsorption against equilibrium concentration ((C_e q_e^{-1}) vs. C_e) as seen in Fig. 14 indicates that endrin adsorption onto zeolite, MOF-199 and MOF-199@ZH obeys the Langmuir model. The Langmuir constants q_o and k_L, determined from the slope and intercept of the plot, are presented in Table 3. The calculated values for q_o indicate MOF-199@ZH has a slightly higher capacity for endrin adsorption compared to zeolite and MOF-199.

The Freundlich isotherm [58] is applicable for non-ideal adsorption on heterogeneous surfaces with multi-layer sorption, is expressed in the subsequent equation

$$\log q_e = \log K_f + (1/n)\log C_e \quad (7)$$

where K_f is related to the adsorption capacity of the adsorbent (mg g^{-1} (L mg^{-1}) $^{1/n}$) and n indicates sorption favorability [59]. The linear plot of the Freundlich isotherm for endrin adsorption onto zeolite, MOF-199 and MOF-199@ZH is documented in Table 3. The best fit kinetic and isotherm a model of composite material (MOF-199@ZH) is shown in Fig. 14.

4. Conclusions

The study concluded that convenient one pot and efficient solvothermal method was used for the synthesis of MOF-199@ZH composites. The successful synthesis of composite was identified by the prominent vibrations observed at 400–1600 cm^{-1} and octahedral geometry was revealed by XRD. Individual zeolite particles showed semicircular shaped that aligned into regular particles coupled with MOF-199. EDX determined presence of silicon, oxygen, aluminum, carbon, and copper confirmed co-existence of MOF-199 and zeolite in composite. The synthesized composite was applied as potential adsorbent for the removal of endrin from aqueous solution and revealed efficacy in the following order:

Zeolite < MOF-199 < MOF-199@ZH

The statistical modeling proposed best agreement (R^2 > 0.99) of experimental data to Langmuir isotherm and pseudo- second order kinetics.

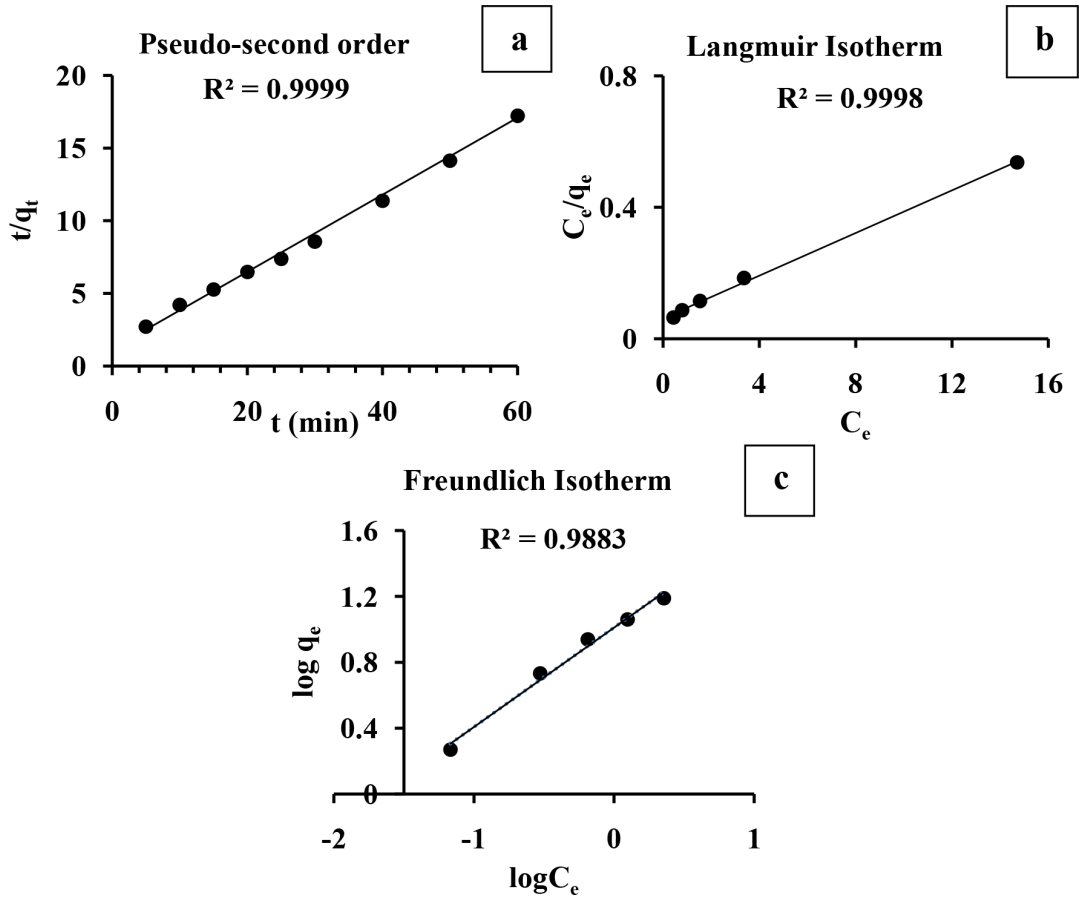

Fig. 14. Statistical modeling and kinetics for MOF-199@ZH (a) pseudo-second order, (b) Langmuir (c) Freundlich.

References

[1] A. Zafirakou, Sustainable urban water management, in: City Networks, Springer, 2017, pp. 227–258.

[2] E. Ayranci, N. Hoda, Adsorption kinetics and isotherms of pesticides onto activated carbon-cloth, Chemosphere, 60 (2005) 1600–1607.

[3] Y.-F. Guan, J.-Z. Wang, H.-G. Ni, E.Y. Zeng, Organochlorine pesticides and polychlorinated biphenyls in riverine runoff of the Pearl River Delta, China: assessment of mass loading, input source and environmental fate, Environ. Pollut., 157 (2009) 618–624.

[4] H. Nakata, M. Kawazoe, K. Arizono, S. Abe, T. Kitano, H. Shimada, W. Li, X. Ding, Organochlorine pesticides and polychlorinated biphenyl residues in foodstuffs and human tissues from China: status of contamination, historical trend, and human dietary exposure, Arch. Environ. Contam. Toxicol., 43 (2002) 0473–0480.

[5] B. Poon, C. Leung, C. Wong, M. Wong, Polychlorinated biphenyls and organochlorine pesticides in human adipose tissue and breast milk collected in Hong Kong, Arch. Environ. Contam. Toxicol., 49 (2005) 274–282.

[6] Y.-F. Jiang, X.-T. Wang, Y. Jia, F. Wang, M.-H. Wu, G.-Y. Sheng, J.-M. Fu, Occurrence, distribution and possible sources of organochlorine pesticides in agricultural soil of Shanghai, China, J. Hazard. Mater., 170 (2009) 989–997.

[7] R.M. Loewy, L.B. Monza, V.E. Kirs, M.C. Savini, Pesticide distribution in an agricultural environment in Argentina, J. Environ. Sci. Health, Part B, 46 (2011) 662–670.

[8] S.O. Wandiga, Use and distribution of organochlorine pesticides. The future in Africa, Pure Appl. Chem., 73 (2001) 1147–1155.

[9] M.A. Khan, M. Iqbal, I. Ahmad, M.H. Soomro, M.A. Chaudhary, Economic evaluation of pesticide use externalities in the cotton zones of Punjab, Pakistan [with comments], The Pakistan Development Review, 2002, pp. 683-698.

[10] S.A.-M.-A.-S. Eqani, R.N. Malik, A. Mohammad, The level and distribution of selected organochlorine pesticides in sediments from River Chenab, Pakistan, Environmental Geochem. Health, 33 (2011) 33–47.

[11] M.I. Tariq, S. Afzal, I. Hussain, N. Sultana, Pesticides exposure in Pakistan: a review, Environ. Int., 33 (2007) 1107–1122.

[12] N.K. Gopalan, S. Chenicherry, Fate and distribution of organochlorine insecticides (OCIs) in Palakkad soil, India, Sustain. Environ. Res., 28 (2018) 179–185.

[13] V. Zitko, Chlorinated pesticides: Aldrin, DDT, endrin, dieldrin, mirex, in: Persistent Organic Pollutants, Springer, 2003, pp. 47–90.

[14] S.A. Greene, R.P. Pohanish, Sittig's handbook of pesticides and agricultural Chemicals, 2005.

[15] D. Mohan, A. Sarswat, Y.S. Ok, C.U. Pittman Jr, Organic and inorganic contaminants removal from water with biochar, a renewable, low cost and sustainable adsorbent–a critical review, Bioresour. Technol., 160 (2014) 191–202.

[16] D.D. Asouhidou, K.S. Triantafyllidis, N.K. Lazaridis, K.A. Matis, S.-S. Kim, T.J. Pinnavaia, Sorption of reactive dyes from aqueous solutions by ordered hexagonal and disordered mesoporous carbons, Micropor. Mesopor. Mater., 117 (2009) 257–267.

[17] Y. Matsui, Y. Fukuda, T. Inoue, T. Matsushita, Effect of natural organic matter on powdered activated carbon adsorption of trace contaminants: characteristics and mechanism of competitive adsorption, Water Res., 37 (2003) 4413–4424.

[18] A. Robers, M. Figura, P. Thiesen, B. Niemeyer, Desorption of odor–active compounds by microwaves, ultrasound, and water, AIChE J., 51 (2005) 502–510.
[19] D.B. Radić, M.M. Stanojević, M.O. Obradović, A.M. Jovović, Thermal analysis of physical and chemical changes occuring during regeneration of activated carbon, Thermal Sci., (2016) 48–48.
[20] G. Zhu, Synthesis of Zeolite@ MOF nanoporous composites as bifunctional catalysts, in, 2014.
[21] V.K. Saini, J. Pires, Development of metal organic framework-199 immobilized zeolite foam for adsorption of common indoor VOCs, J. Environ. Sci., 55 (2017) 321–330.
[22] S. Baradaran, M. Sohrabi, P.M. Bijani, S. Javid, Effect of pH on the synthesis of ZSM-5 zeolite using TEOS and performance of H-ZSM-5 catalyst in propane aromatization. Proc. 15th Iranian National Congress of Chemical Engineering (IChEC 2015).
[23] M. Kasture, P. Niphadkar, S. Kate, P. Godbole, K. Patil, G. Chaphekar, P. Joshi, Influence of silica and alumina source materials on the physicochemical characteristics of crystalline zeolite beta, in: Studies in Surface Science and Catalysis, Elsevier, 2004, pp. 3081–3087.
[24] T.V.N. Thi, C.L. Luu, T.C. Hoang, T. Nguyen, T.H. Bui, P.H.D. Nguyen, T.P.P. Thi, Synthesis of MOF-199 and application to CO_2 adsorption, Adv. Nat. Sci.: Nanosci. Nanotechnol., 4 (2013) 035016.
[25] C. Petit, T.J. Bandosz, Enhanced adsorption of ammonia on metal-organic framework/graphite oxide composites: analysis of surface interactions, Adv. Funct. Mater., 20 (2010) 111–118.
[26] M. Gougazeh, J.-C. Buhl, Synthesis and characterization of zeolite A by hydrothermal transformation of natural Jordanian kaolin, J. Assoc. Arab Univ. Basic Appl. Sci., 15 (2014) 35–42.
[27] M. Treacy, J. Higgins, Collection of simulated XRD powder patterns for zeolites. Published on behalf of the Structure Commission of the 'International Zeolite Association', Powder Patterns, 203, 204 (2001).
[28] Q.M. Wang, D. Shen, M. Bülow, M.L. Lau, S. Deng, F.R. Fitch, N.O. Lemcoff, J. Semanscin, Metallo-organic molecular sieve for gas separation and purification, Micropor. Mesopor. Mater., 55 (2002) 217–230.
[29] P. Chowdhury, C. Bikkina, D. Meister, F. Dreisbach, S. Gumma, Comparison of adsorption isotherms on Cu-BTC metal organic frameworks synthesized from different routes, Micropor. Mesopor. Mater., 117 (2009) 406–413.
[30] K. Schlichte, T. Kratzke, S. Kaskel, Improved synthesis, thermal stability and catalytic properties of the metal-organic framework compound Cu3 (BTC) 2, Micropor. Mesopor. Mater., 73 (2004) 81–88.
[31] H. Dathe, E. Peringer, V. Roberts, A. Jentys, J.A. Lercher, Metal organic frameworks based on Cu^{2+} and benzene-1, 3, 5-tricarboxylate as host for SO_2 trapping agents, Comptes Rendus Chimie., 8 (2005) 753–763.
[32] G. Liu, L. Li, X. Huang, S. Zheng, D. Xu, X. Xu, Y. Zhang, H. Lin, Determination of triazole pesticides in aqueous solution based on magnetic graphene oxide functionalized MOF-199 as solid phase extraction sorbents, Micropor. Mesopor. Mater., 270 (2018) 258–264.
[33] C. Petit, J. Burress, T.J. Bandosz, The synthesis and characterization of copper-based metal–organic framework/graphite oxide composites, Carbon., 49 (2011) 563–572.
[34] Z. Huo, X. Xu, Z. Lv, J. Song, M. He, Z. Li, Q. Wang, L. Yan, Y. Li, Thermal study of NaP zeolite with different morphologies, J. Thermal Anal. Calorim., 111 (2013) 365–369.
[35] G. Zeng, Y. Chen, L. Chen, P. Xiong, M. Wei, Hierarchical cerium oxide derived from metal-organic frameworks for high performance super capacitor electrodes, Electrochim. Acta, 222 (2016) 773–780.
[36] K. Sun, L. Li, X. Yu, L. Liu, Q. Meng, F. Wang, R. Zhang, Functionalization of mixed ligand metal-organic frameworks as the transport vehicles for drugs, J. Colloid Interf. Sci., 486 (2017) 128–135.
[37] J. He, Y. Zhang, Q. Pan, J. Yu, H. Ding, R. Xu, Three metal-organic frameworks prepared from mixed solvents of DMF and HAc, Micropor. Mesopor. Mater., 90 (2006) 145–152.
[38] S.K. Papageorgiou, E.P. Kouvelos, E.P. Favvas, A.A. Sapalidis, G.E. Romanos, F.K. Katsaros, Metal–carboxylate interactions in metal–alginate complexes studied with FTIR spectroscopy, Carbohyd. Res., 345 (2010) 469–473.
[39] C. Petit, B. Levasseur, B. Mendoza, T.J. Bandosz, Reactive adsorption of acidic gases on MOF/graphite oxide composites, Micropor. Mesopor. Mater., 154 (2012) 107–112.
[40] H.-L. Zubowa, H. Kosslick, D. Müller, M. Richter, L. Wilde, R. Fricke, Crystallization of phase-pure zeolite NaP from MCM-22-type gel compositions under microwave radiation, Micropor. Mesopor. Mater., 109 (2008) 542–548.
[41] L.V. Rees, S. Chandrasekhar, Hydrothermal reaction of kaolinite in presence offluoride ions at pH < 10, Zeolites, 13 (1993) 534–541.
[42] S. Loera-Serna, M.A. Oliver-Tolentino, M. de Lourdes López-Núñez, A. Santana-Cruz, A. Guzmán-Vargas, R. Cabrera-Sierra, H.I. Beltrán, J. Flores, Electrochemical behavior of [Cu3(BTC)2] metal–organic framework: the effect of the method of synthesis, J. Alloys Comp., 540 (2012) 113–120.
[43] Y. Li, J. Miao, X. Sun, J. Xiao, Y. Li, H. Wang, Q. Xia, Z. Li, Mechanochemical synthesis of Cu-BTC@ GO with enhanced water stability and toluene adsorption capacity, Chem. Eng. J., 298 (2016) 191–197.
[44] H. Li, Z. Lin, X. Zhou, X. Wang, Y. Li, H. Wang, Z. Li, Ultrafast room temperature synthesis of novel composites Imi@ Cu-BTC with improved stability against moisture, Chem. Eng. J., 307 (2017) 537–543.
[45] K. Shrivas, A. Ghosale, P. Maji, Advanced nanomaterials for the removal of chemical substances and microbes from contaminated and waste water, in: advanced nanomaterials for water engineering, treatment, and hydraulics, IGI Global, 2017, pp. 127–161.
[46] A.S. Al-Barrak, S.M. Elsaid, Pesticides removal from drainage waste water using some agricultural wastes, Pak. J. Biol. Sci., 8 (2005) 374–378.
[47] B. Seyhi, P. Drogui, P. Gortares-Moroyoqui, M.I. Estrada–Alvarado, L.H. Alvarez, Adsorption of an organochlorine pesticide using activated carbon produced from an agro–waste material, J. Chem. Technol. Biotechnol., 89 (2014) 1811–1816.
[48] H. El Bakouri, J. Morillo, J. Usero, A. Ouassini, Potential use of organic waste substances as an ecological technique to reduce pesticide ground water contamination, J. Hydrology, 353 (2008) 335–342.
[49] F.A. Ansari, M. Alam, Kinetics and equilibrium isotherm studies of endrin and o, p DDT Adsorption on Low Cost Adsorbent, Parthenium hysterophorous Activated with Nitric Acid and Methanol.
[50] S. Kaur, S. Rani, R.K. Mahajan, Adsorption kinetics for the removal of hazardous dye congo red by biowaste materials as adsorbents, J. Chemistry, 2013 (2012).
[51] M.E. Argun, S. Dursun, C. Ozdemir, M. Karatas, Heavy metal adsorption by modified oak sawdust: Thermodynamics and kinetics, J. Hazard. Mater., 141 (2007) 77–85.
[52] J. Zhu, S. Wei, H. Gu, S.B. Rapole, Q. Wang, Z. Luo, N. Haldolaarachchige, D.P. Young, Z. Guo, One-pot synthesis of magnetic graphene nanocomposites decorated with core@ double-shell nanoparticles for fast chromium removal, Environ. Sci. Technol., 46 (2011) 977–985.
[53] M. Ajmal, R.A.K. Rao, R. Ahmad, M.A. Khan, Adsorption studies on Parthenium hysterophorous weed: removal and recovery of Cd (II) from wastewater, J. Hazard. Mater., 135 (2006) 242–248.
[54] S. Lagergren, About the theory of so-called adsorption of soluble substances, Sven. Vetenskapsakad. Handingarl, 24 (1898) 1–39.
[55] Y.-S. Ho, G. McKay, Pseudo-second order model for sorption processes, Process Biochem., 34 (1999) 451–465.

[56] J. Lalley, C. Han, X. Li, D.D. Dionysiou, M.N. Nadagouda, Phosphate adsorption using modified iron oxide-based sorbents in lake water: kinetics, equilibrium, and column tests, Chem. Eng. J., 284 (2016) 1386–1396.
[57] I. Langmuir, The adsorption of gases on plane surfaces of glass, mica and platinum, J. Amer. Chem. Soc., 40 (1918) 1361–1403.
[58] H. Freundlich, Über die adsorption in lösungen, Zeitschrift für physikalische Chemie, 57 (1907) 385–470.
[59] M. Dávila-Jiménez, M. Elizalde-González, A. Peláez-Cid, Adsorption interaction between natural adsorbents and textile dyes in aqueous solution, Colloids Surfaces A: Physicochem. Eng. Asp., 254 (2005) 107–114.